CASE 49

Direct-Injection Diesel Injector Optimization

Abstract: Delphi Automotive Systems is entering the direct-injection diesel business, which requires a significant shift in technologies from the current diesel injection approach. The injector itself is the key to mastering this goal, and its high sensitivity to sources of variation makes robust engineering a valuable approach to optimization. A robust engineering dynamic experiment based on a numerical model of the injector allowed us to achieve (1) a 4.46-dB improvement in the SN ratio through parameter design, representing a reduction of about 40% in the variability of the quantity injected; (2) an improvement of about 26% in the manufacturing process end-of-line first-time quality (percentage of good injectors at the end of the line) predicted; and (3) the generation of tolerance design-based charts to support manufacturing tolerance decisions and reduce cost further. This robust engineering case study shows that cost-effective and informative robust engineering projects can be conducted using good simulation models, with hardware being used to confirm results.

1. Introduction

The common rail direct-injection diesel fuel system is an important technology for Delphi. For this reason, a product and process engineering team, dedicated to the design and implementation of the best possible common rail system with respect to both product and process, was set up at the European Technical Center. The direct-injection diesel common rail system is comprised of the following core components of the engine management system:

- ❏ Injectors
- ❏ High-pressure pump
- ❏ Fuel rail and tubes
- ❏ High-pressure sensor
- ❏ Electronic control module
- ❏ Pressure control system

The main challenge with diesel common rail systems as opposed to indirect diesel injection systems is the continuous high operating pressures. Current common rail systems are designed to operate with pressure levels of 1350 to 1600 bar.

Figure 1 shows a sample injector and its key variability sources. The injector is the most critical and the most complex element of the system. A diesel common rail system will not be successful if the injectors are not "world class" in term of quality and reliability.

Problem

The injector complexity is due to very tight manufacturing tolerances and challenging customer requirements for quantity injected. These issues are confirmed by the problems reported by our competitors. Some of them experienced very high scrap levels in production. An alternative approach is to build quality into the product at an early stage of design.

Injector operation is affected by the following sources of variability: (1) other elements of the engine and (2) the management system.

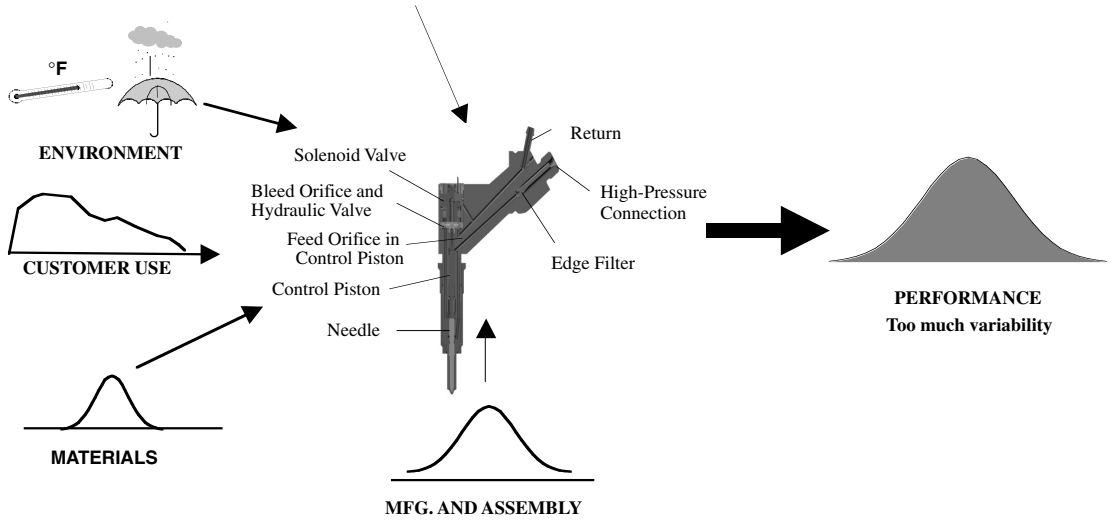

Figure 1
Injector and key variability sources

Objectives and Approach to Optimization

The optimization process followed the flowchart in Figure 2. A simulation model was developed, improved, and used to perform the orthogonal array experiments. Because of the very high confidence level in the simulation model (see Figure 7), we decided to use hardware only for the confirmation runs.

The main deliverables assigned to this optimization process were:

- ❏ Reduced part-to-part and shot-to-shot variation in quantity injected
- ❏ Part-to-part variation among several injectors
- ❏ Shot-to-shot variation from one injection to the next within the same injector
- ❏ Decreased sensitivity to manufacturing variation and ability to reduce cost by increasing component tolerances as appropriate
- ❏ Graphical tools to increase understanding of downstream quality drivers in the design

The following labeling is used in the experiment:

A: control factor for parameter design

A': control factor variation considered as a noise factor

A'': control factor included in the tolerance design

2. Simulation Model Robustness

A direct-injection diesel injector for a common rail system is a complex component with high-precision parts and very demanding specifications. To simulate such a component means representing the physical transient interactions of a coupled system, including a magnetic actuator, fluid flows at very high pressure, possibly with cavitation phenomena, and moving mechanical parts. The typical time scale for operation is a few microseconds to a few milliseconds.

Because pressure wave propagation phenomena are very important in the accurate representation of injector operation, the simulation code cannot be limited to the injector itself but must include the common rail and the connection pipe from the rail to the injector (Figure 3)

The rail and the connection line are standard hydraulic elements in which the model calculates wave propagation using classical methods for solving wave equations. The internal structure of the injector is illustrated in Figure 4. We can distinguish two hydraulic circuits and one moving part (plus the mobile part of the control valve). The first hydraulic circuit feeds the control volume at the common rail high pressure through a calibrated orifice. The pressure, P_C, in the control volume is controlled by

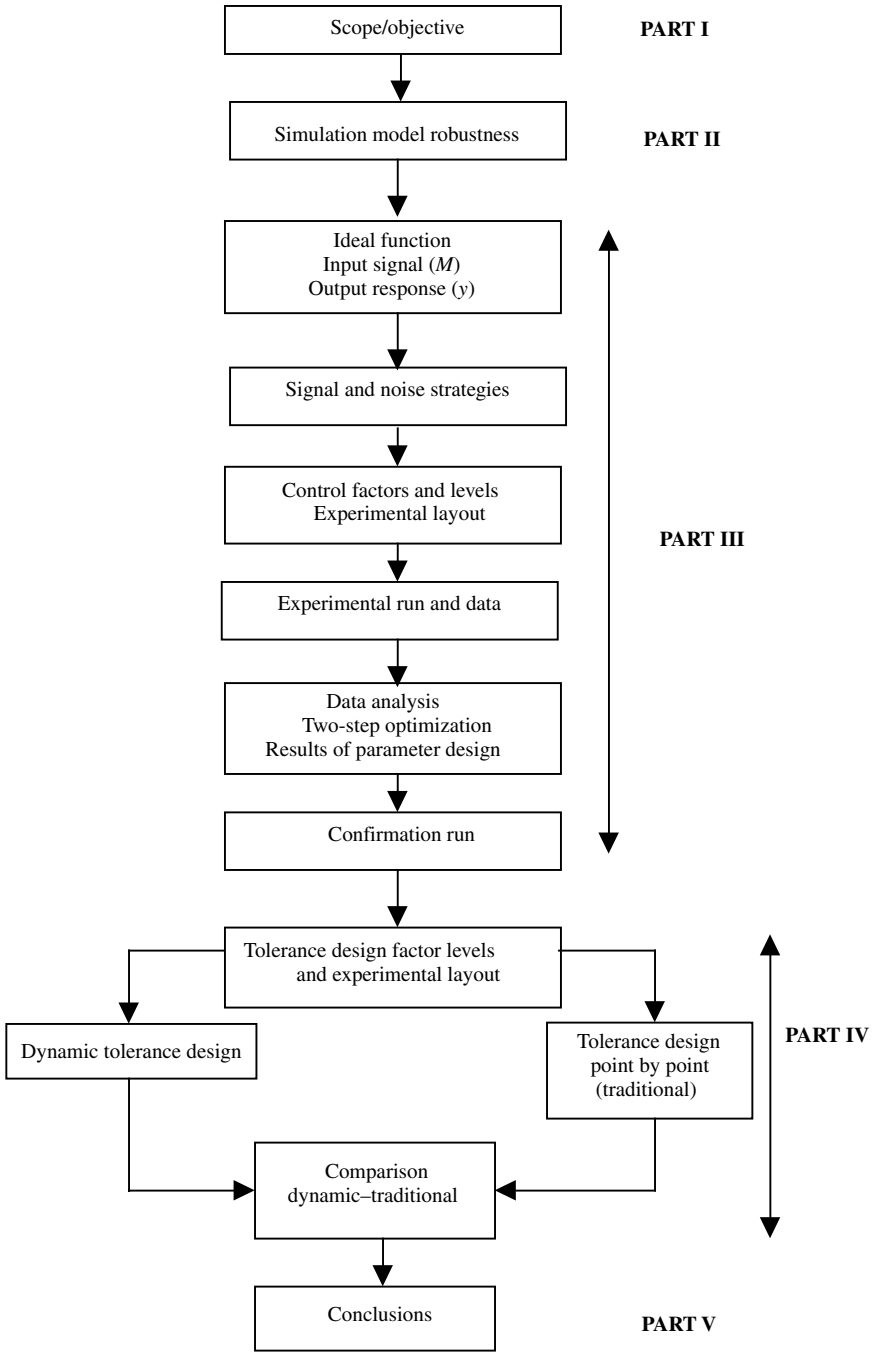

Figure 2
Optimization process

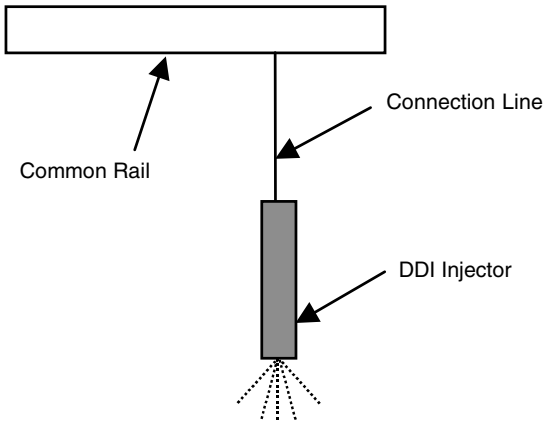

Figure 3
Modeled system

activating the electromechanical control valve and bleeding off a small amount of fluid. The duration of electrical activation, called the *pulse width*, is calculated by the engine control module (ECM), depending on driver demand, rail pressure, and engine torque needs. The other hydraulic circuit feeds the nozzle volume at a pressure, P_N, that remains close to common rail pressure. Using internal sealing, the area stressed by the pressure is larger on the control volume side than on the nozzle side. Thus, as long as P_C and P_N remain equal, the needle is pushed against the nozzle seat and the injector is closed. To start an injection event, the control valve is activated, which lowers the pressure in the control chamber until the force balance on the needle changes sign. Then the needle moves up, and injection occurs. To close the injector, the control valve is closed and the pressure builds up again in the control chamber until the force balance on the needle changes sign again and the needle moves down and closes.

The structure of the mathematical model of the injector can be deduced from its physical structure (Figure 5). Three submodels are coupled:

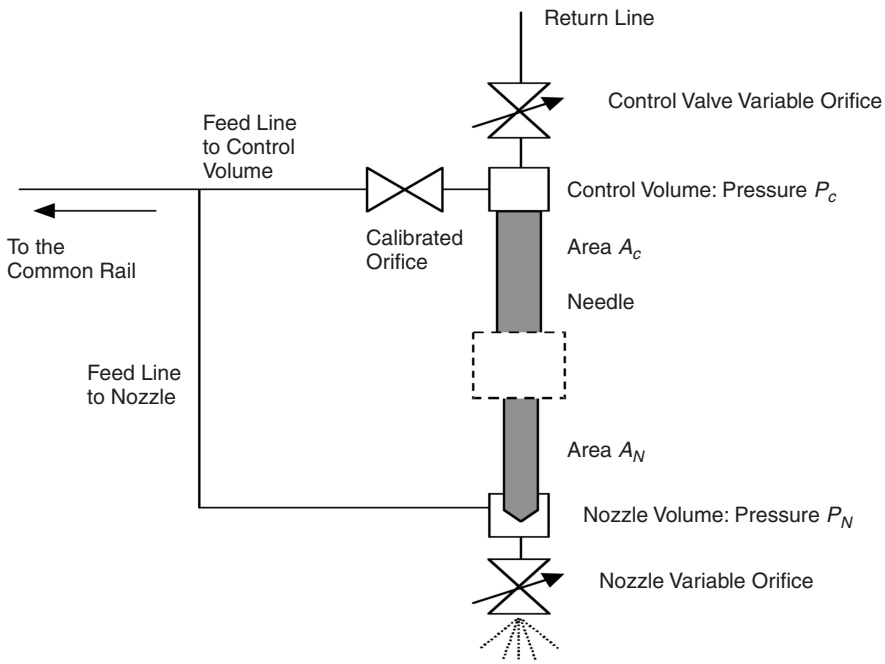

Figure 4
Injector

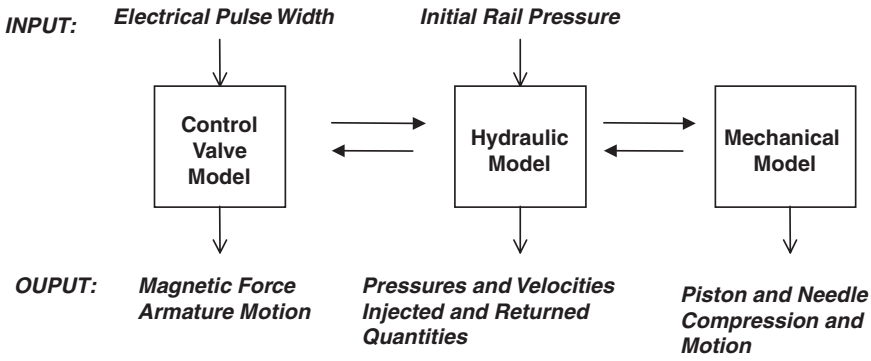

Figure 5
Mathematical model

1. Electromechanical control valve
2. Hydraulic circuits
3. Mechanical moving parts

Model inputs are as follows:

- ❏ Duration of electrical activation of electromagnetic actuator
- ❏ Rail pressure

Model outputs include time variation of the following elements:

- ❏ Magnetic force
- ❏ Fuel pressure and velocity in lines
- ❏ Flows through orifices
- ❏ Displacement of moving parts

The behavior of a direct-injection diesel injector can be characterized by a *mapping*, which gives the fuel quantity injected versus pulse width and rail pressure (Figure 6). Given the initial rail pressure and the pulse width, the model is expected to predict accurately the quantity of fuel that should be injected.

Approach to Optimization

The difficulty in building and then optimizing such a model is that some features have a very strong effect on the results. Imprecision about their model representation can affect results in an unacceptable way. Experimental investigations have been used to thoroughly study the characteristics of internal flows

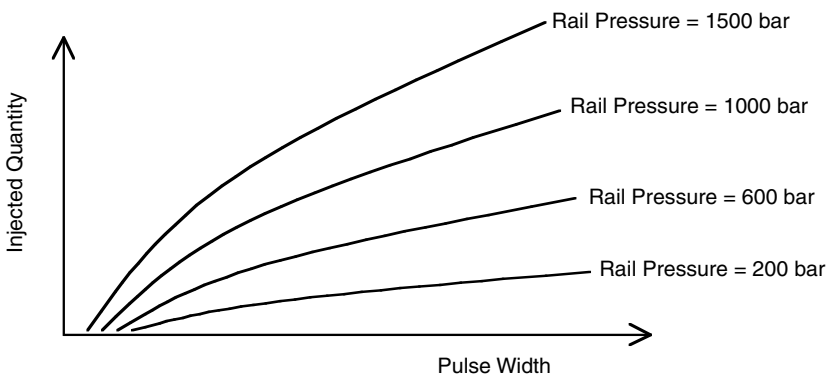

Figure 6
Quantity injected versus pulse width for various rail pressure levels

in key parts such as the control valve and the nozzle, for instance. From these experiments, empirical equations have been fitted and then implemented in the model. Finally, the transient nature of the flows is also a problem because most of the experiments are done statically.

In the end, after implementing the most realistic physical representation of variables, based either on experiments or on theoretical calculation, injector model optimization is a feedback loop between model results and experimentally observable injection parameters, such as injected quantity, injection timing, and control valve displacement. Engineering judgment is then necessary to assess the cause of any discrepancy and to improve or even change the physical representation of variables shown to be inadequate.

Results

Figure 7 shows the correlation between model and experiment for quantity injected, for rail pressures and pulse widths covering the full range of injector operation, and for three different injectors with different settings of control factor values. The agreement between model and hardware is good over the full range of operation. Figure 7 is the basis of the high confidence level we have in the model outputs.

3. Parameter Design

Ideal Function

The direct-injection diesel injector has several performance characteristics:

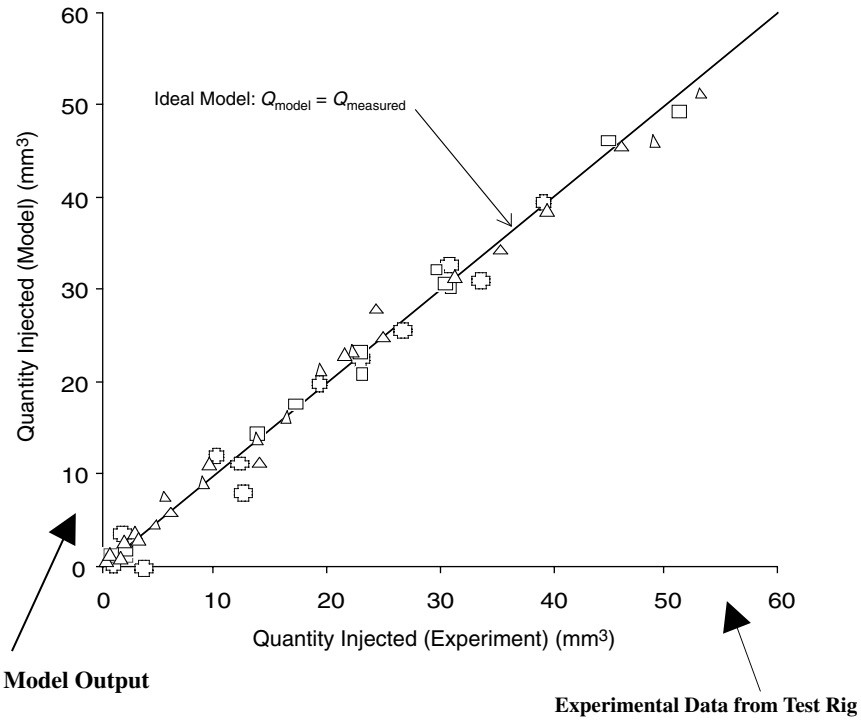

Figure 7
Comparison model data versus experimental data for various rail pressure, pulse width, and injector control factor settings (□, reference; Δ, control factors *A, B, G, E*, and *F* changed; O, control factors *A, B, G, E*, and *I* changed)

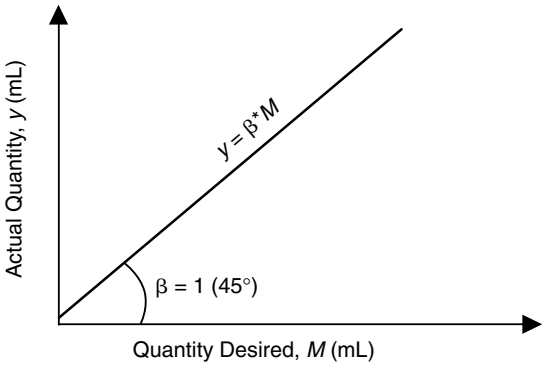

Figure 8
Ideal function

- ❏ Recirculated quantity
- ❏ Total opening time
- ❏ Delay of main injection
- ❏ Quantity injected

In the traditional approach, these performance characteristics would require individual optimizations and trade-off based on experimental results. In such a case, the power of a carefully chosen ideal function is invaluable. For an injection system, the customer requirement can be expressed as the quantity of fuel required for good combustion at a given operating point. By considering the customer need as a signal, we can compute through the simulation model, under noise conditions, what the actual injector will deliver. This last value is the *y*-axis of the ideal function. A perfect injector will have a slope of 1, with the actual quantity equal to the value desired (Figure 8). A design that exhibits the ideal function shown in Figure 8 is likely to be acceptable for any of the performance characteristics listed above.

Signal and Noise Strategies

Five levels of injected quantity desired were selected based on customer specifications: 2, 5, 15, 25, and 40 mL. Table 1 shows the impact of the noise factors

Table 1
Noise factors

Noise Factor	Level	Level	Relationship with Quantity Injected	Compounded Noise Level 1 (N_1)	Compounded Noise Level 2 (N_2)	Rationale[a]
B′	−10	+10	+	1	2	Mfg.
C′	−5	+5	+	1	2	Age
D′	−2	+2	+	1	2	Mfg., Age
E′	−3	+3	−	2	1	Mfg., Age
F′	−3	+3	−	2	1	Age
G′	−3	+3	+	1	2	Mfg., Age
H′	−4	+4	−	2	1	Age
I′	−30	+30	+	1	2	Mfg.
J′	−3	+3	+	1	2	Age
L	0.6	1	+	1	2	Mfg., Age
M	−10	+10	+	1	2	System
N	0	0.03	+	1	2	Mfg.
O	2	5	+	1	2	Mfg.

[a] Mfg., manufacturing variation; Age, aging; System, influence of other components.

Table 2
Control factors and levels (%)[a]

	Level		
Factor	**1**	**2**	**3**
A	−16.6	*X*	+16.6
B	−11.1[b]	*X*	+11.1
C	−16.6	*X*	+16.6
D	−11.1[b]	*X*	+11.1
E	−28.6	*X*	+28.6[b]
F	−18.5	*X*	+18.5
G	−18.2	*X*	+22.7[b]
H	+33.3	*X*	+66.6
I	−11.1	*X*	+11.1[b]
J	−8.62	*X*	+6.9[b]
K	−2.3	*X*	+2.3[b]

[a] *X* is a reference value. An L_{27} (3^{13}) orthogonal array was used to perform the experiment. Two columns were unused (see Figure 9).
[b] Current design level.

on the quantity injected. A (+) indicates that an increase in the noise factor will increase the injected quantity (direct relationship). A (−) indicates that a decrease in the noise factor will increase the injected quantity (inverse relationship).

The compounded noise level 1 (N_1) groups all the noise factor levels that have the effect of reducing the quantity injected. The compounded noise level 2 (N_2) groups the noise factor levels that have the effect of increasing the quantity injected.

B', C' ... , J' are noise factors obtained by considering variation (from manufacturing or other sources) of the corresponding control factors. *L*, *M*, *N*, and *O* are noise factors not derived from control factors. We expect these noises to be present during product use.

Control Factors and Levels

Table 2 shows control factors and levels for the experiment. Table 3 shows the experimental layout.

Data Analysis and Two-Step Optimization

The data were analyzed using the dynamic SN ratio:

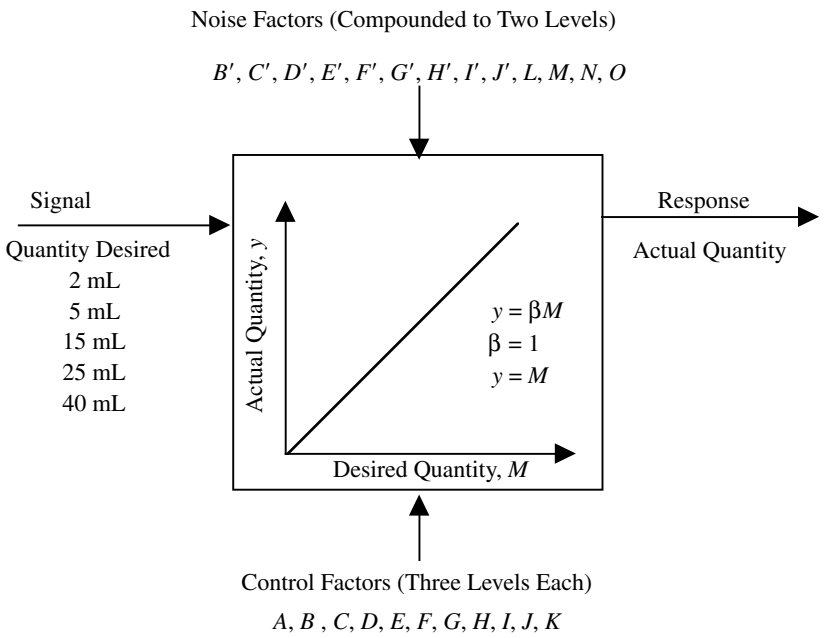

Figure 9
Parameter design

Table 3
Experimental layout

	Control Factor Array												Signal											
													2 mL		5 mL		15 mL		25 mL		40 mL			
No.	*A*	*B*	*C*	*D*	*E*	*F*	*G*	*H*	*I*	*J*	*K*	12	13	N_1	N_2	N_1	N_2	N_1	N_2	N_1	N_2	N_1	N_2	S/N	β
1	1	1	1	1	1	1	1	1	1	1	1	1	1												
2	1	1	1	1	2	2	2	2	2	2	2	2	2												
3	1	1	1	1	3	3	3	3	3	3	3	3	3												
⋮																									
25	3	3	2	1	1	3	2	3	2	1	2	1	3												
26	3	3	2	1	2	1	3	1	3	2	3	2	1												
27	3	3	2	1	3	2	1	2	1	3	1	3	2												

$$\eta = 10 \log \frac{S_\beta - V_e}{rV_e}$$

where S_β is the sum of squares of distance between zero and the least squares best-fit line (forced through zero) for each data point, V_e the mean square (variance), and r the effective divider. See Figure 10 for the SN and sensitivity analyses. Note the SN *Y*-axis values are all negative and expressed in decibels in the figure. See Tables 4 and 5 for further results.

Confirmation

The model in Table 6 confirms the expected improvement with a slight difference. Neither the optimum nor the current design combinations were part of the control factor orthogonal array. The initial hardware testing on the optimized configuration showed promising results. See Figure 11 for results.

Results

B and *C* are control valve parameters. The design change on these parameters suggested by parameter design is likely to improve injected quantity, part-to-part, and shot-to-shot variation. The simulation model confirms these improvements. Hardware confirmation is ongoing. *A*, *D*, *E*, *G*, *H*, *I*, *J* are hydraulic parameters. Implementing the changes suggested by parameter design will decrease our sensitivity to most of the noise factors and to pressure fluctuations in the system.

An improvement in SN ratio can be translated directly into a reduction in variability:

$$\text{variability improvement} = \left(\tfrac{1}{2}\right)^{\text{gain}/6} \times \text{initial variability}$$

where gain is the SN ratio gain in decibels; in our case, the model confirmed gain is 4.46 dB (Table 6). We are making an almost 40% reduction in variability from the initial design.

The slope of the ideal function is distributed normally. The tolerance on the slope can be obtained from the tolerances at each signal point of injection (Table 7 and Figure 12).

From the tolerances on β, and assuming a normal distribution, we can draw a curve to relate end-of-line scrap level or first-time quality (FTQ) (Figure 13) to the deviation from the target, β. This is not meant to reject the loss function approach. Rather, it is to quantify the reduction in part rejection (and therefore cost avoidance) at the end of the assembly line if we implement the recommendations from parameter design. The end-of-assembly line first-time quality (FTQ) is calculated by the formula

$$\text{FTQ} = \frac{\text{number of injectors within tolerances}}{\text{total number of injectors produced}}$$

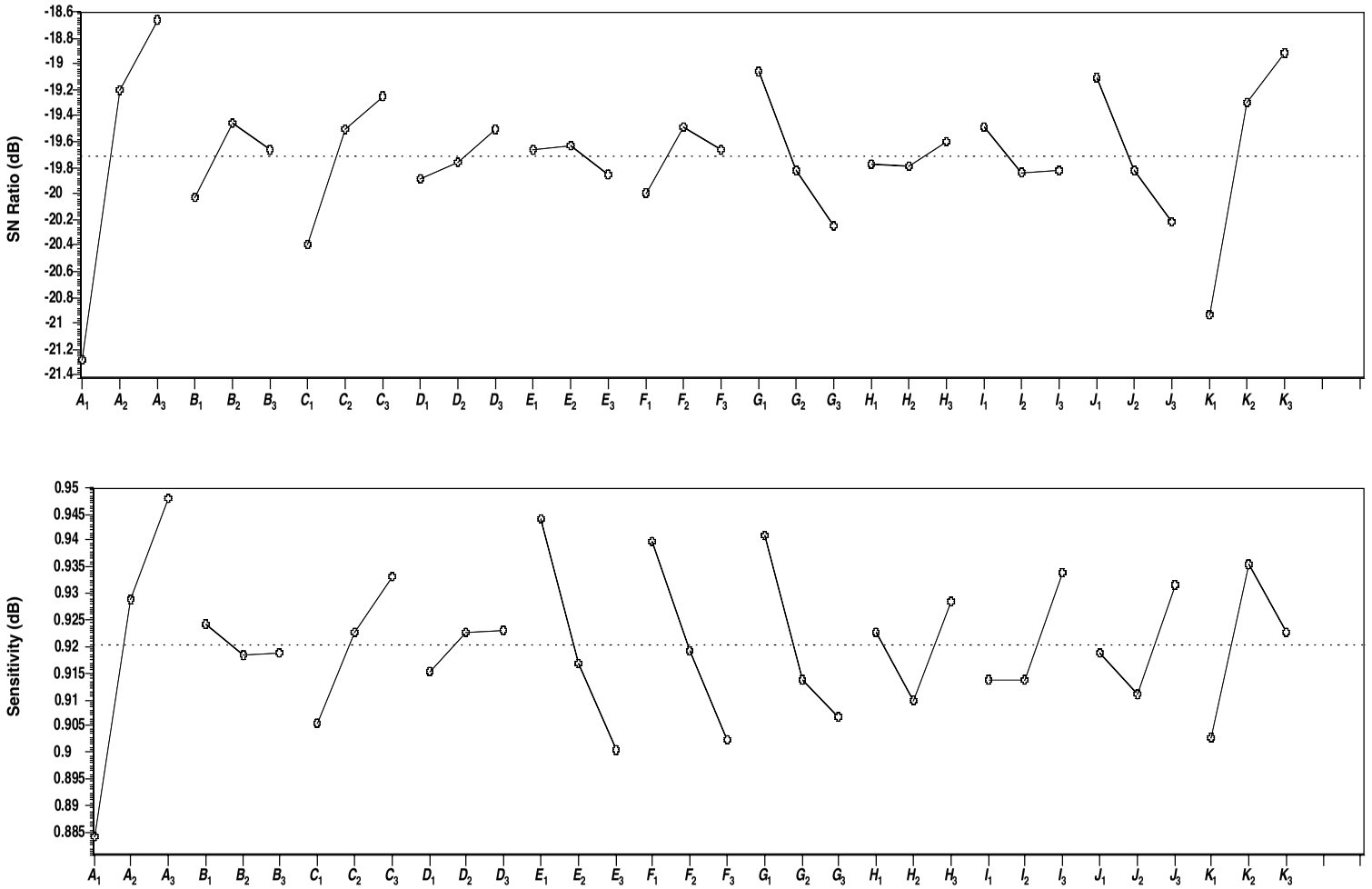

Figure 10
SN ratio and sensitivity plots

Table 4
Two-step optimization

	Factor										
	A	***B***	***C***	***D***	***E***	***F***	***G***	***H***	***I***	***J***	***K***
Initial design	A_2	B_1	C_1	D_1	E_3	F_2	G_3	H_2	I_3	J_3	K_3
SN maximization (first step)	A_3	B_2	C_3	D_3	$E_?$	F_2	G_1	H_3	I_1	J_1	K_3
Adjustment for beta (second step)					E_1						
Optimized design	A_3	B_2	C_3	D_3	E_1	F_2	G_1	H_3	I_1	J_1	K_3
	Design change required						Design change required				

The figure identifies FTQ. If β is the observed slope, $\mu = 1$ is the mean, z is the number of standard deviations away from the mean, and $\phi(z)$ is the standard cumulative normal distribution function.

In Figure 13, σ is the observed standard deviation on β, σ_i the standard deviation on β before parameter design, and σ_{opt} the standard deviation after parameter design.

$$\beta_{min} = 0.945$$

$$\beta_{max} = 1.054$$

$$Z_2 = \frac{\beta_{max} - 1}{\sigma} \quad \text{and} \quad Z_1 = \frac{\beta_{min} - 1}{\sigma}$$

$$\begin{aligned} FTQ &= \phi(Z_2) - \phi(Z_1) = [1 - \phi(Z_1)] - \phi(Z_1) \\ &= 1 - 2\phi(Z_1) \\ &= 1 - 2\phi\left(\frac{\beta_{max} - 1}{\sigma}\right) \end{aligned}$$

Table 5
Prediction

Design	SN (dB)	β (Slope)
Initial	−20.7118	0.8941
Optimized	−15.0439	1.0062
Gain	+5.66	0.1121

So FTQ is a function of the observed standard deviation of β. If the standard deviation of β from the initial design is σ_i,

$$\sigma_{opt} = \sqrt{0.6\sigma_i^2} = 0.77\sigma_i$$

considering the 40% reduction in variability from parameter design, the standard deviation of β from the optimized design after parameter design is the predicted end-of-line fraction of good parts is obtained through the curve in Figure 14. We simulate the improvement on FTQ with two different values of σ_i on β. It is hard to know the current value of σ_i, but we know that the optimized standard deviation is 0.77 σ_i.

Possible FTQ improvement in percent with a standard deviation on β from the initial design equal to σ_i is shown in Table 8.

4. Tolerance Design

Tolerance design is traditionally conducted with nondynamic responses. With a dynamic robust experiment, this is not optimal and can result in endless trade-off discussions. The ranked sensitivity to tolerances might be different from one signal point to another. A way to solve this is the use of dynamic tolerance design. In this robust design experiment, tolerance design was performed both on a signal point basis and on a dynamic basis. In dynamic tolerance design, optimization is based on β instead of the quantity injected. The tolerance on β is obtained by considering the tolerances at each signal

Table 6
Model confirmation

	Predicted		Confirmed			
			Model		Hardware	
Design	SN (dB)	β	SN (dB)	β	SN	β
Initial	−20.7118	0.8941	−20.2644	0.9150	Ongoing	Ongoing
Optimum	−15.0439	1.0062	−15.8048	0.9752	Ongoing	Ongoing
Gain	5.66	0.1121	4.46	0.06		

point and drawing a best-fit line. This ensures a more comprehensive tolerance design. (Figure 15). To illustrate, we perform tolerance design with the two approaches and compare them in Tables 9 and 10.

Signal Point by Signal Point Tolerance Design

Factors and Experimental Layout We used a three-level tolerance design with 13 parameters. Therefore, we will once again use an L_{27} array. The signal point–based tolerance design is performed using the data in the corresponding signal point column. Analysis of variance (ANOVA) for each injection point is shown in Table 11. The percent contribution is shown in Figure 16 (injection point 1: 2 mL desired). (The ANOVA was performed at each signal point.)

Loss Function For the signal point tolerance design, the loss function was nominal-the-best on the quantity injected. The calculations in Table 12 were performed for each signal point. In the table, $\%r$ is the percent contribution of the design parameter to the injected quantity variability. L_{tc} is the total current loss in dollars in the Taguchi loss function. σ_{pc} is the design parameter current standard deviation or its current tolerance level. σ_t is the current total output standard deviation, considering the variation of all design parameters. σ_p is a variable representing the standard deviation of a design parameter. L_{cp} is the current fraction of the total loss caused by the corresponding parameter. The higher the contribution percentage ($\%r$), the higher the L_{cp} value for a given design parameter. FTQ is the first-time quality (end of assembly line). L_p is the loss caused by a design parameter given any value of the parameter standard deviation σ_p (L_p is a function of σ_p). See also Figure 17 and Table 13. K is the proportional constant of the loss function.

$$K = \frac{A_0}{\Delta_0^2} = 9.18C$$

A_0 = base average injector cost in dollars = $\$C$

Δ_0 = specification on quantity injected = 0.33 mL at 1σ

V_T = current total variance from ANOVA = 0.7542

$L_{\text{tc}} = KV_T = \$6.9235C$

Figure 18 shows the loss/cost as a function of each parameter.

Dynamic Tolerance Design

The control factor settings are the same as in the signal point tolerance design. In this case the response becomes the β from each combination. We use a nominal-the-best approach with the target β = 1 (ideal function). Results are shown in Table 14.

Dynamic Analysis of Variance β replaces the quantity injected. The target for β is 1 in this case. The boundaries for injector first-time quality correspond here to the upper and lower lines that we can draw on each signal point based on customer specifications (see Figure 12). The ANOVA is given in Table 15 and the percent contribution in Figure 19.

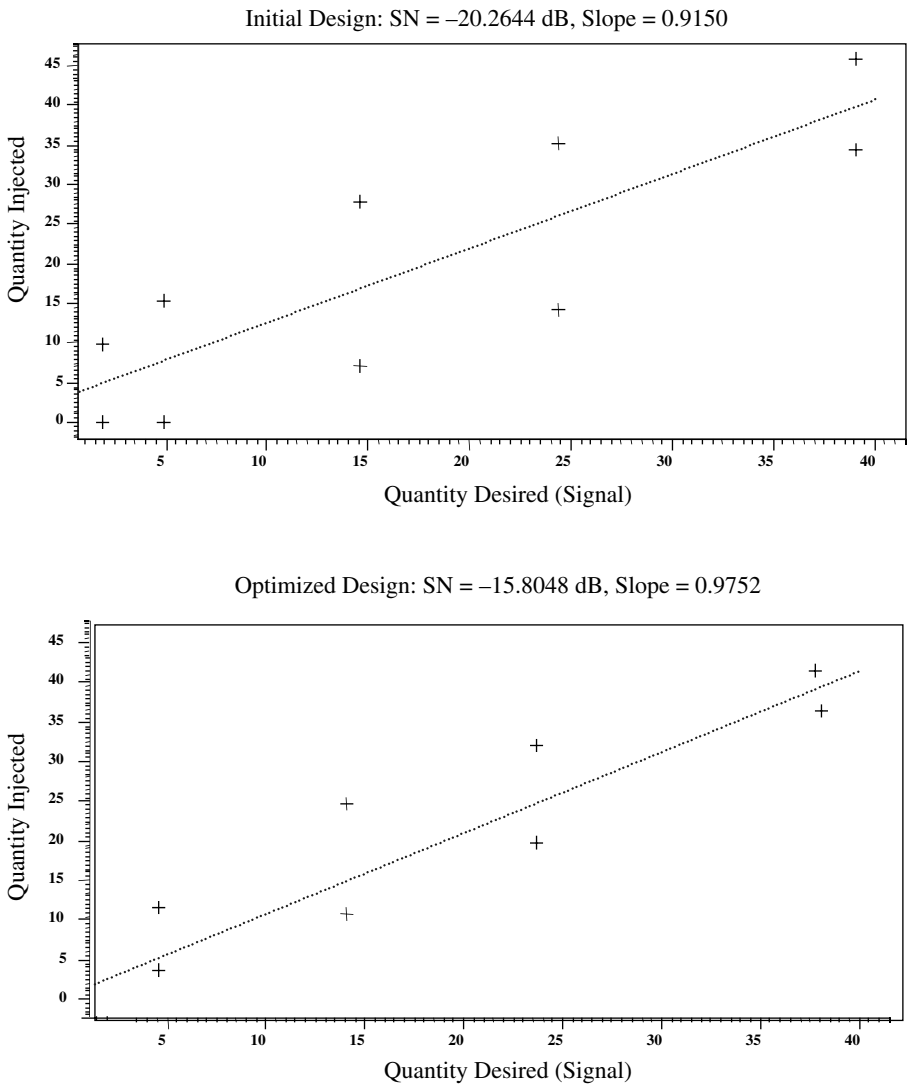

Figure 11
Graphical results of initial design compared to optimized design

Dynamic Loss Function The current loss distribution is shown in Table 16 and the dynamic tolerance design in Figure 20.

Dynamic characteristic: slope β. This is the same as signal point by signal point tolerance design. The response is β in this case; $\%r$ is the percent contribution of the design parameter on the β variability; and K is the proportional constant of the loss function.

$$K = \frac{A_0}{\Delta_0^2} = 2500°\text{C}$$

A_0 = average injector cost in dollars = $\$C$

Table 7
Slope specifications

Quantity Desired	Minimum Quantity Acceptable (at 3σ)	Target	Maximum Quantity Acceptable (at 3σ)
2	1	2	3
25	21.5	25	28.5
40	36.5	40	43.5
β (slope)	0.945 (at 3σ)	1	1.054 (at 3σ)

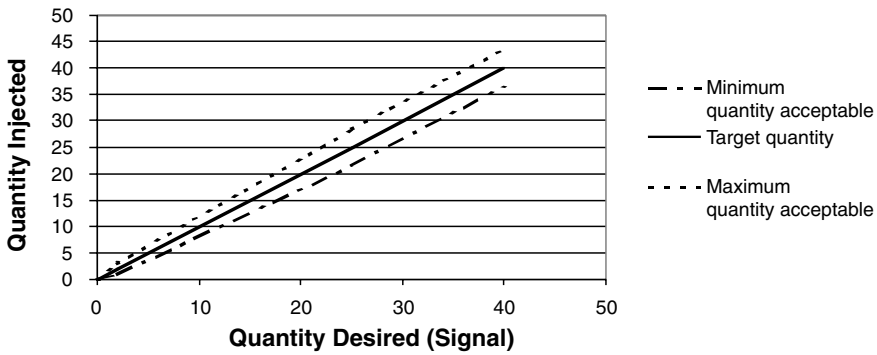

Figure 12
Slope tolerance

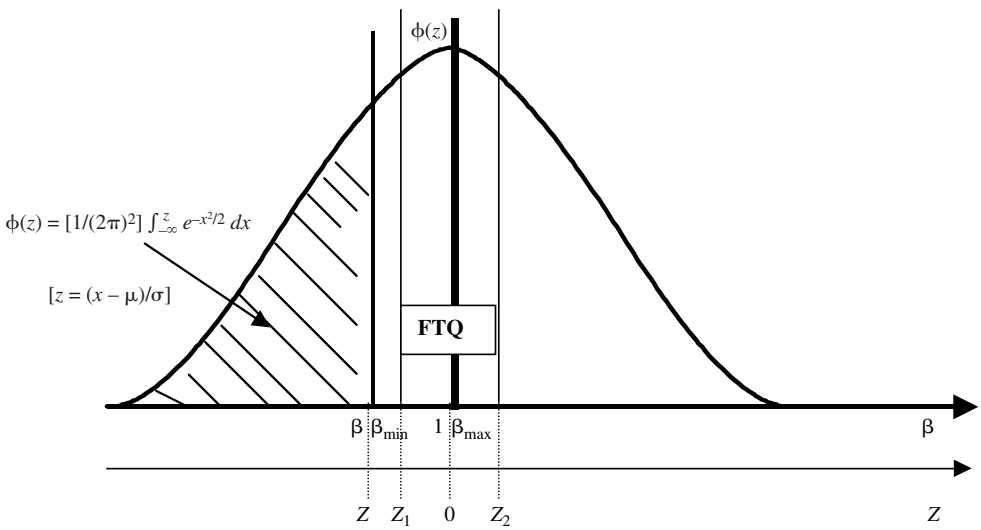

Figure 13
FTQ representation

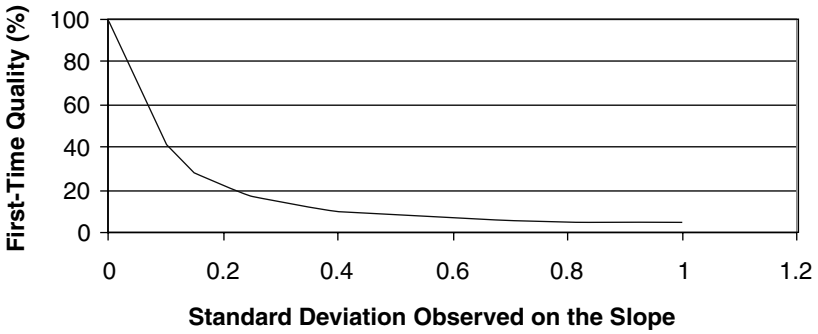

Figure 14
End-of-line FTQ as a function of the standard deviation observed on β

Table 8
End-of-line FTQ as a function of the standard deviation on the slope

σ_i	σ_{opt}	FTQ_i (%)	FTQ_{opt} (%)	ΔFTQ (%)	Gain (on FTQ %) Initial to Optimized (%)
0.10	0.076	41	52	11	26
0.05	0.038	72	84	12	16

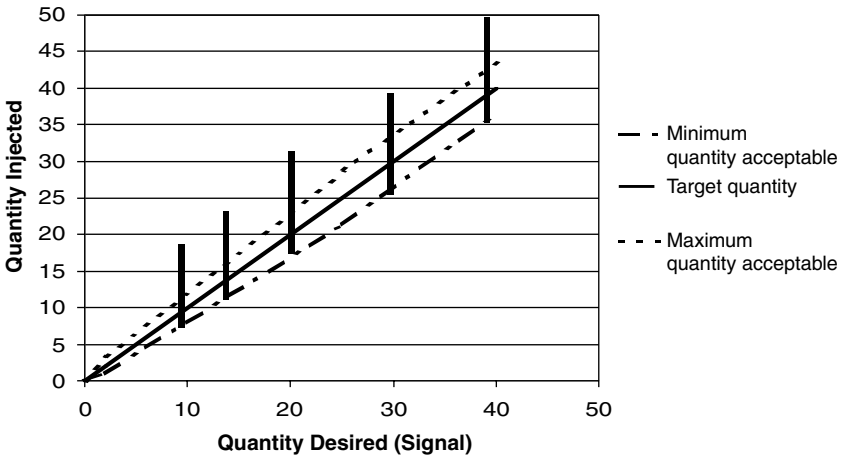

Figure 15
Tolerance design: signal point versus dynamic

Table 9
Factors and levels for tolerance design[a]

Factor	Level 1 $X - \sqrt{3/2}\,\sigma$	Level 2 X	Level 3 $X + \sqrt{3/2}\,\sigma$	Current σ (%)
A″				3.810
B″				3.704
C″				2.381
D″				1.333
E″				0.010
F″				0.004
G″				0.002
H″				2.667
I″				6.250
J″				0.002
K″				0.114
L				0.022
M				2.632

[a] X is the optimized level of each design parameter; σ is the current tolerance of each design parameter.

Table 10
Tolerance design experimental layout

	Tolerance Factor													Signal				
No.	*A″*	*B″*	*C″*	*D″*	*E″*	*F″*	*G″*	*H″*	*I″*	*J″*	*K″*	*L*	*M*	2 mL	5 mL	15 mL	25 mL	40 mL
1	1	1	1	1	1	1	1	1	1	1	1	1	1					
2	1	1	1	1	2	2	2	2	2	2	2	2	2					
3	1	1	1	1	3	3	3	3	3	3	3	3	3					
⋮																		
25	3	3	2	1	1	3	2	3	2	1	2	1	3					
26	3	3	2	1	2	1	3	1	3	2	3	2	1					
27	3	3	2	1	3	2	1	2	1	3	1	3	2					

Table 11
ANOVA for signal point 1

Source	d.f.	*S*	*V*	*F*	*S*	ρ
A″	2	2.6413	1.3206	15.9851	2.4760	12.63
B″	2	4.3410	2.1705	26.2721	4.1758	21.30
C″	2	0.0672	0.0336	—	—	—
D″	2	2.2450	1.1225	13.5872	2.0798	10.61
E″	2	0.3953	0.1977	—	—	—
F″	2	0.9158	0.4579	5.5426	0.7506	2.83
G″	2	1.0480	0.5240	6.3427	0.8828	4.50
H″	2	0.0332	0.0166	—	—	—
I″	2	0.6072	0.3036	3.6750	0.4420	2.25
J″	2	0.5165	0.2582	3.1257	0.3512	1.79
K″	2	2.0346	1.0173	12.3134	1.8693	9.53
L	2	4.2696	2.1348	25.8403	4.1044	20.93
M	2	0.4940	0.2470	2.9899	0.3288	1.68
e_1						
(*e*)	6	0.4957	0.0826	—	2.1480	10.95
Total	26	19.6087	0.7542			

(*e*) is pooled error.

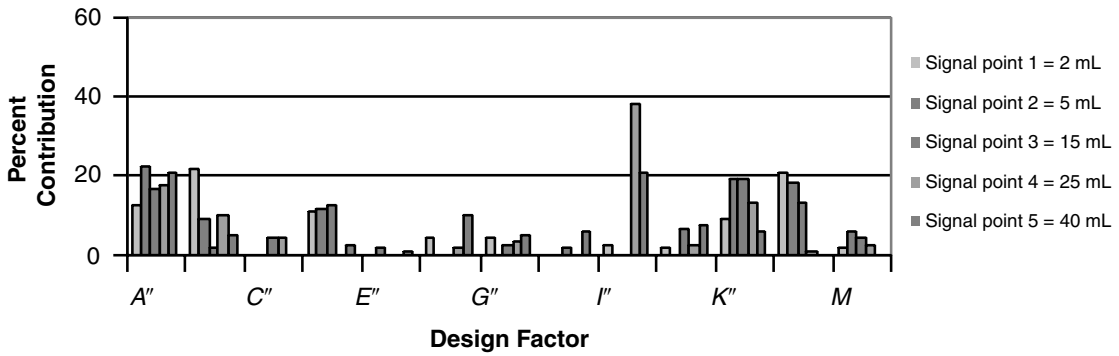

Figure 16
Percent contribution of design factors to variability per signal point

Table 12
Percent contribution of design factors to variability (signal point 1: 2 mL desired)

Factor	r (%)	L_{tc} (c)	Current, σ_{pc}	L_{cp} (c)
A''	12.63	6.9235	3.81	0.8744381
B''	21.30	6.9235	3.70	1.474706
C''	0	6.9235	2.38	0
D''	10.61	6.9235	1.33	0.7345834
E''	0	6.9235	0.01	0
F''	3.83	6.9235	0.00	0.2651701
G''	4.5	6.9235	0.00	0.3115575
H''	0	6.9235	2.67	0
I''	2.25	6.9235	6.25	0.1557788
J''	1.79	6.9235	0.00	0.1239307
K''	9.53	6.9235	0.11	0.6598096
L	20.93	6.9235	0.02	1.449089
M	1.68	6.9235	2.63	0.1163148

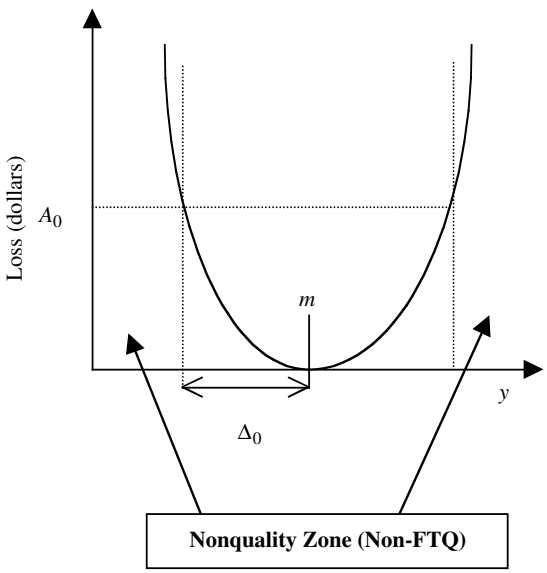

Figure 17
Taguchi loss function

Δ_0 = specification on $\beta = 0.02$ at 1σ

V_T = current total variance from ANOVA = 0.0012

$L_{tc} = KV_T = \$3C$

Comparison of dynamic tolerance design and signal point tolerance design. The total loss with dynamic tolerance design was almost half of the total loss when tolerance design was conducted signal point by signal point. We do not have a precise explanation for this finding. The percent contributions of the

Table 13
Summary of current total loss for some signal points

Signal Point (mL)	Current Total Loss
2	$6.9235C
25	$0.5541C
40	$0.5541C

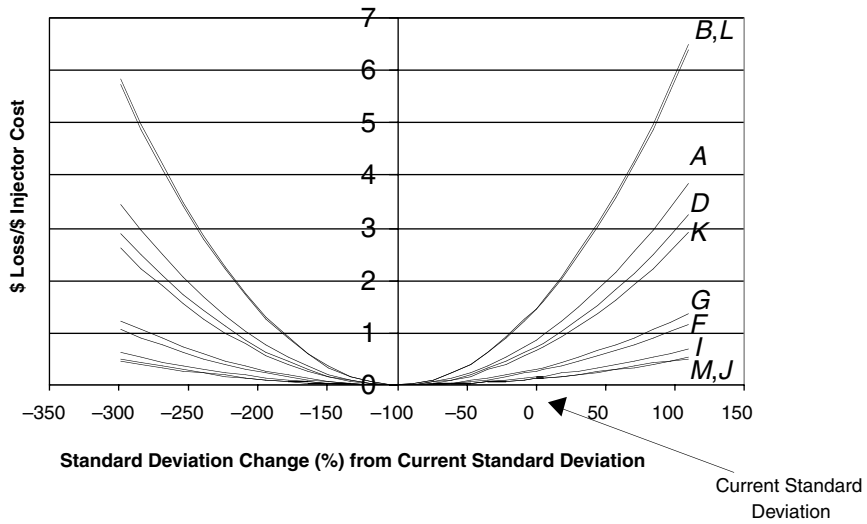

Figure 18
Chart to support manufacturing tolerance decision making (signal point 1: 2 mL)

design parameters at each signal point (see Figure 16) were difficult to use for decision making, due to the complexity of trade-off. We found it easier to consider the global percent contributions obtained from dynamic tolerance design (see Figure 19).

5. Conclusions

A gain of 4.46 dB in the SN ratio was realized in the modeled performance of the direct-injection diesel injector. This gain represents a reduction of about

Table 14
Experimental layout for dynamic tolerance design

	Tolerance Factor													
No.	***A″***	***B″***	***C″***	***D″***	***E″***	***F″***	***G″***	***H″***	***I″***	***J″***	***K″***	***L***	***M***	
1	1	1	1	1	1	1	1	1	1	1	1	1	1	β_1
2	1	1	1	1	2	2	2	2	2	2	2	2	2	β_2
3	1	1	1	1	3	3	3	3	3	3	3	3	3	β_3
⋮														⋮
25	3	3	2	1	1	3	2	3	2	1	2	1	3	β_{25}
26	3	3	2	1	2	1	3	1	3	2	3	2	1	β_{26}
27	3	3	2	1	3	2	1	2	1	3	1	3	2	β_{27}

Table 15
Dynamic tolerance design ANOVA

Source	d.f.	*S*	*V*	*F*	*S′*	*ρ*
A″	2	0.0117	0.0059	35.4725	0.0114	35.50
B″	2	0.0010	0.0005	2.9348	0.0006	1.99
C″	2	0.0066	0.0033	20.1535	0.0063	19.73
D″	2	0.0001	0.0000	—	—	—
E″	2	0.0006	0.0003	—	—	—
F″	2	0.0002	0.0001	—	—	—
G″	2	0.0000	0.0000	—	—	—
H″	2	0.0005	0.0003	—	—	—
I″	2	0.0029	0.0015	8.9340	0.0026	8.17
J″	2	0.0038	0.0019	11.5096	0.0035	10.82
K″	2	0.0005	0.0003	—	—	—
L	2	0.0004	0.0002	—	—	—
M	2	0.0037	0.0018	11.0911	0.0033	10.39
e_1						
e_2						
(*e*)	14	0.0023	0.0002	—	0.0043	13.39
Total	26	0.0320	0.0012			

(*e*) is pooled error.

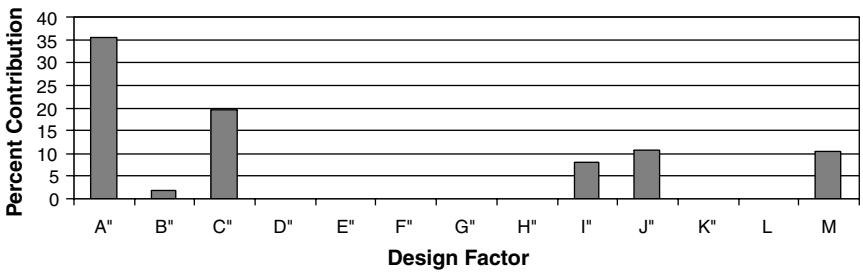

Figure 19
Percent contribution of design factors on the slope (dynamic tolerance design)

Table 16
Total current loss distribution among parameters

Factor	r (%)	L_{tc} (c)	L_{cp} (c)
A''	35.5	3	1.065
B''	1.99	3	0.0597
C''	19.73	3	0.5919
D''	0	3	0
E''	0	3	0
F''	0	3	0
G''	0	3	0
H''	0	3	0
I''	8.17	3	0.2451
J''	10.82	3	0.3246
K''	0	3	0
L	0	3	0
M	10.39	3	0.3117

40% in the variability in the quantity injected. We anticipate that the variability reduction will translate to a 16 to 26% increase of the fraction of parts inside tolerances for quantities injected at the end of the manufacturing line.

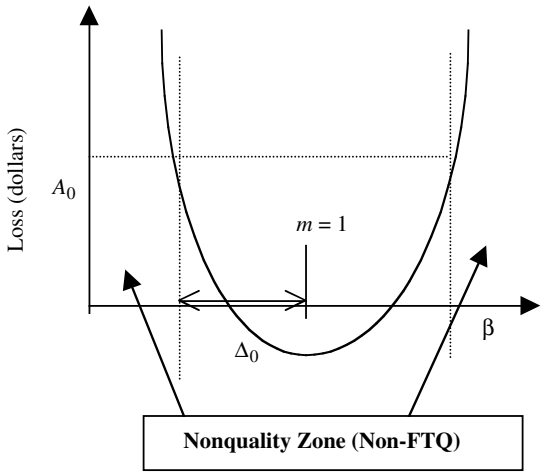

Figure 20
Taguchi loss function for dynamic tolerance design

Several charts were developed to support manufacturing process tolerance decision making. As information on tolerance upgrade or degrade cost is made available, the charts will be used to reduce cost further by considering larger tolerances where appropriate.

Recommendations

We recommend the use of dynamic tolerance design for dynamic responses. Optimization at individual signal points may not always lead to a clear and consistent design recommendation. This case study proposes a solution for a nominal–the-best situation for tolerance design. A standardized approach needs to be developed to cover dynamic tolerance design.

Hardware cost is one of the roadblocks to Taguchi robust design implementation. The development of good simulation models will help overcome this roadblock while increasing the amount of good information that one can extract from the projects. With a good model, we can conduct parameter design and tolerance design with a great number of control factors. We are also able to simulate control factor manufacturing variation as noise factors. The ability to consider manufacturing variation is an important advantage compared to full hardware-based robust engineering. Hardware confirmation should be conducted to ascertain the results and should not lead to a surprise if a good robustness level is achieved up front on the simulation model.

Acknowledgments We would like to acknowledge Dr. Jean Botti, Dr. Martin Knopf, Aparicio Gomez, Mike Seino, Carilee Cole, Giulio Ricci from Delphi Automotive Systems and Shin Taguchi and Alan Wu from the American Supplier Institute for their technical support.

References

John Neter, 1983. *Applied Linear Regression Models.* Homewood, IL: Richard D. Irwin.

Yuin Wu and Alan Wu, 1998. *Taguchi Methods for Robust Design.* Livonia, Michigan; ASI Press.

This case study is contributed by Desire Djomani, Pierre Barthelet, and Michael Holbrook.